Proc. Natl. Acad. Sci. USA
Vol. 95, pp. 4847–4852, April 1998
Biochemistry

Crystal structure of troponin C in complex with troponin I fragment at 2.3-Å resolution

DMITRY G. VASSYLYEV*, SOICHI TAKEDA*, SOICHI WAKATSUKI†, KAYO MAEDA*, AND YUICHIRO MAÉDA*‡

*International Institute for Advanced Research, Central Research Laboratories, Matsushita Electric Industrial Co., Ltd., 3-4 Hikaridai, Seika, Kyoto, 619-02, Japan; and †European Synchrotron Radiation Facility, BP 220, F-38043 Grenoble Cedex, France

Communicated by Carolyn Cohen, Brandeis University, Waltham, MA, February 17, 1998 (received for review November 20, 1997)

ABSTRACT **Troponin (Tn), the complex of three subunits (TnC, TnI, and TnT), plays a key role in Ca^{2+}-dependent regulation of muscle contraction. To elucidate the interactions between the Tn subunits and the conformation of TnC in the Tn complex, we have determined the crystal structure of TnC (two Ca^{2+} bound state) in complex with the N-terminal fragment of TnI (TnI_{1-47}). The structure was solved by the single isomorphous replacement method in combination with multiple wavelength anomalous dispersion data. The refinement converged to a crystallographic *R* factor of 22.2% (R_{free} = 32.6%). The central, connecting α-helix observed in the structure of uncomplexed TnC (TnC_{free}) is unwound at the center (residues Ala-87, Lys-88, Gly-89, Lys-90, and Ser-91) and bent by 90°. As a result, TnC in the complex has a compact globular shape with direct interactions between the N- and C-terminal lobes, in contrast to the elongated dumb-bell shaped molecule of uncomplexed TnC. The 31-residue long TnI_{1-47} α-helix stretches on the surface of TnC and stabilizes its compact conformation by multiple contacts with both TnC lobes. The amphiphilic C-end of the TnI_{1-47} α-helix is bound in the hydrophobic pocket of the TnC C-lobe through 38 van der Waals interactions. The results indicate the major difference between Ca^{2+} receptors integrated with the other proteins (TnC in Tn) and isolated in the cytosol (calmodulin). The TnC/TnI_{1-47} structure implies a mechanism of how Tn regulates the muscle contraction and suggests a unique α-helical regulatory TnI segment, which binds to the N-lobe of TnC in its Ca^{2+} bound conformation.**

The regulation of skeletal and cardiac muscle contraction is associated with a Ca^{2+}-dependent structural transition in the muscle thin filament—the complex of actin, tropomyosin, and troponin (Tn) (1–3). The signals induced by the variations of the Ca^{2+} concentration are transferred to the other components of the thin filament through the Ca^{2+} receptor, Tn (4, 5). Tn consists of three distinct subunits: TnC, TnI, and TnT. TnC is the Ca^{2+}-binding subunit. TnT binds to tropomyosin, and thereby anchors Tn to the muscle thin filament. The binding of Ca^{2+} to TnC facilitates the release of inhibitory segment of TnI from the actin molecule, thus triggering the actomyosin Mg^{2+}-ATPase (6–8). This process is regulated by TnC in a Ca^{2+}-dependent manner. At the binding of Ca^{2+}, the N-lobe of TnC undergoes a structural transformation from the "closed" state to the "open" Ca^{2+}-bound form (9–11). These alterations of the TnC N-lobe facilitate the release of the regulatory region of TnI from the thin filament binding site and ensure its preferential binding to TnC, which relieves the inhibition of the actomyosin Mg^{2+}-ATPase.

The crystal structure of TnC_{free}, determined at an acidic pH (5.0), revealed a dumb-bell shaped molecule that consists of two N- and C-terminal lobes (N- and C-lobes) connected by a long central α-helix (12, 13). Each lobe has two Ca^{2+}-binding helix–turn–helix motifs, known as EF-hands. Under physiological conditions, the EF-hands in the C-lobe always are occupied by Ca^{2+} or Mg^{2+}, whereas the N-lobe has lower affinity for Ca^{2+}, and its EF-hands can be filled with Ca^{2+} only at the release of Ca^{2+} into the sarcoplasm. Thus, it now is believed that the C-lobe plays a structural role in TnC, whereas the N-lobe is directly involved in the regulation of muscle contraction.

Although the structure of TnC_{free} has been known for more than a decade, its conformation within Tn, as well as the structural mechanism of how TnC regulates the actomyosin Mg^{2+}-ATPase activity, remains obscure. To elucidate the functional role and the conformation of TnC in Tn, we have determined the crystal structure of TnC in complex with TnI_{1-47}.

MATERIALS AND METHODS

Protein Preparation and Crystallization. In the present study, to avoid N-terminal heterogeneity, TnC was expressed by using pMal-c2 (New England Biolabs) as a fusion protein, which was cleaved by factor Xa after purification. The recombinant TnC molecule used in the present work has an extra Met residue at the N terminus, which is not in the peptide sequence of the rabbit skeletal muscle TnC (SWISS-PROT entry P02586). Therefore, in this report, this Met is omitted from the numbering of the TnC amino acid residues. The sequence of rabbit TnC was aligned with the chicken TnC sequence (91% of homology), used for the comparison in the present study, so that the rabbit amino acid with number N corresponds to the residue numbered (N+3) in the chicken sequence. The TnC/TnI_{1-47} complex was prepared and crystallized as described previously, with minor modifications (14). It was found that the nonisomorphism between the native and heavy atom derivative crystals (14) is not induced by the heavy atom soaking, but should be addressed to the nonisomorphism of different native crystals. The crystals used in this study belong to the space group $P3_221$, with the unit cell dimensions $a = b = 46.9$ Å, $c = 152.3$ Å, and with a solvent content of 35%.

Data Collection. The data for the native TnC/TnI_{1-47} complex and its PCMBS (*p*-chloro-mercuribenzenesulfonate) derivative at three distinct wave lengths (including one at the absorption edge of the Hg atom) have been collected from the two single frozen crystals (100K) at beam line BM14 (European Synchrotron Radiation Facility, Grenoble). The PCMBS derivative crystal diffracted to only 2.8-Å resolution. The diffraction data were processed with the programs DENZO and SCALEPACK (15) (Table 1). Judging by the unit cell dimensions,

Abbreviations: TN, troponin; PCMBS, *p*-chloro-mercuribenzenesulfonate.

Data deposition: Crystallographic data (coordinates and structure factors) have been deposited at the Protein Data Bank, Biology Department, Brookhaven National Laboratory, Upton, NY 11973 (entry 1A2X).

‡To whom reprint requests should be addressed. e-mail: ymaeda@crl.mei.co.jp.

The publication costs of this article were defrayed in part by page charge payment. This article must therefore be hereby marked "*advertisement*" in accordance with 18 U.S.C. §1734 solely to indicate this fact.

the native and PCMBS derivative crystals were isomorphous to each other.

Structure Determination. All initial attempts to determine the TnC/TnI_{1-47} structure by molecular replacement by using the programs AMORE (16) and X-PLOR (17), and the structure of uncomplexed TnC, as either a whole or its lobes, failed. The structure was solved by using the single isomorphous replacement (SIR) method in combination with the multiple wavelength anomalous dispersion (MAD) technique. The major heavy atom site of the PCMBS derivative was located in both isomorphous and anomalous difference Patterson maps with the RSPS program (16). The heavy atom site was refined by using the MLPHARE program (18) modified by D.G.V. (unpublished work), and three additional minor heavy atom sites were found in the difference Fourier maps. The overall figure of merit was 0.85 at 2.8-Å resolution. The SIR/MAD electron density map then was calculated, and the phases were improved by solvent flattening and histogram matching using the DM program (16). The rough orientation of the TnC lobes (Protein Data Bank entry 1TOP) in the final electron density map was determined manually by using the O program (19). The TnC model then was rebuilt to achieve the best fit to the electron density, and the interlobe linker region and the TnI_{1-47} α-helix were modeled with the O program.

Refinement. The data in the 25- to 10-Å shell were omitted from the refinement because this shell contains a substantial number of overloaded intensities. The *R* factor for the initial model was 48%. The model was refined with the program X-PLOR (17) (Table 1). During the course of refinement, the fraction of residues in the most favorable region of the Ramachandran plot increased from 80% to 88.3%, as indicated by the program PROCHECK (20). No residues were found in the disallowed region of the Ramachandran plot. The average *B* factor of the final model is 43 $Å^2$. Almost all of the modeled residues, including their side chains, are well defined by the electron densities in the final (2Fo-Fc) map.

RESULTS AND DISCUSSION

Structure Determination. The crystal structure of the complex between rabbit skeletal muscle TnC (160 residues, 18 kDa) and TnI_{1-47} has been solved by the single isomorphous replacement/multiple wavelength anomalous dispersion technique (Table 1). The refinement converged to an *R* factor of 22.2% (R_{free} = 32.6%) at 2.3-Å resolution (Table 1). The final model lacks two N-terminal residues of TnC, and two and 14 amino acids from the N- and C-termini of TnI_{1-47}, respectively, probably because these residues are disordered in the crystal.

Structure Description. The conformation of TnC in the TnC/TnI_{1-47} complex is strikingly different from that of TnC_{free}, in which the two lobes are connected by a long α-helix, and thus, the length of the molecule is about 65 Å (12, 13). In the complex, this connecting D/E α-helix is unwound at the center and is transformed into an extended linker between the two TnC lobes. The residues Ala-87, Lys-88, Gly-89, Lys-90, and Ser-91 constitute the linker with the main chain (ϕ, ψ) torsion angles, (−79, 179), (−69, 159), (−92, −171), (−147, 41), and (−50, 146), respectively. All the residues in the linker are well defined by the electron densities, except for the side chain of Lys-88, and their average *B* factor (45 $Å^2$) is very close to the overall average value (43 $Å^2$). The 120° rotation, indicated by the program LSQKAB (16), of the TnC lobes relative to their orientation in the TnC_{free} accompanies the unwinding of the D/E α-helix, which results in a 90° kink (inclination between the two helical axes) between its D- and E-portions. As a result of these alterations, the TnC molecule in the TnC/TnI_{1-47} complex has a compact globular shape, with approximate dimensions of 50 × 30 × 30 Å (Fig. 1*A*). The N- and C-lobes come into close proximity and form a deep narrow interlobe cleft. There are two direct interlobe hydrogen bonds in TnC within the TnC/TnI_{1-47} complex. Only two Ca^{2+}-binding sites (EF-hands) in the C-lobe of TnC in the complex are occupied by Ca^{2+}, whereas the two other EF-hands in the N-lobe are empty (Fig. 1*A*), as was observed in the TnC_{free}

Table 1. Summary of the TnC/TnI_{1-47} complex structure determination

		PCMBS derivative		
Data collection	Native	λ_1 (1.00866 Å)	λ_2 (1.00395 Å)	λ_3 (0.95373 Å)
Resolution (Å)	25.0-2.3	25.0-2.8	25.0-2.8	25.0-2.8
Reflections				
Total (*N*)	37,214	22,050	21,747	23,003
Unique (*N*)	8,870	4,998	4.989	5,091
R_{sym}* (%)	5.0	5.3	6.0	5.1
Completeness (%)	96.3 (82.0)†	94.1	94.4	94.8
R_{iso}‡ (%)	—	22.2	23.2	24.0
Phasing power§	—	3.0	3.1	3.0

Refinement statistics		Stereochemistry	
Resolution (Å)	10.0-2.3 Å	RMSD bond length (Å)	0.01
Number of reflections	8,736	RMSD bond angles (°)	1.28
R_{cryst}¶ (%)	22.2	RMSD improper angles (°)	0.72
R_{free}¶ (%)	32.5		
Number of protein atoms	1,502		
Number of water molecules	89		
Number of calcium ions	2		

*$R_{sym} = \Sigma_{hkl}\Sigma_j | I_j(hkl) - < I(hkl) > | / \Sigma_{hkl}\Sigma_j | < I(hkl) >$, where $I_j(hkl)$ and $< I(hkl) >$ are the intensity of measurement *j* and the mean intensity for the reflection with indices *hkl*, respectively.

†The completeness of reflections with $I > 3\sigma(I)$ is shown in brackets.

‡$R_{iso} = \Sigma_{hkl} || F_{der}(hkl) | - | F_{nati}(hkl) || / \Sigma_{hkl} | F_{nati}(hkl) |$, where $F_{der}(hkl)$ and F_{nati} (hkl) are the structure factors of the heavy atom derivative and the native for the reflection with indices *hkl*, respectively.

§Phasing power = $< F_h > /E$, where $<F_h>$ is the root mean square heavy-atom structure factor and E is the residual lack of closure error.

¶$R_{cryst,free} = \Sigma_{hkl} || F_{calc}(hkl) | - | F_{obs}(hkl) || / \Sigma_{hkl} | F_{obs} |$, where the crystallographic *R* factor is calculated including and excluding the refinement reflections. The free reflections constituted 7% of the total number of reflections.

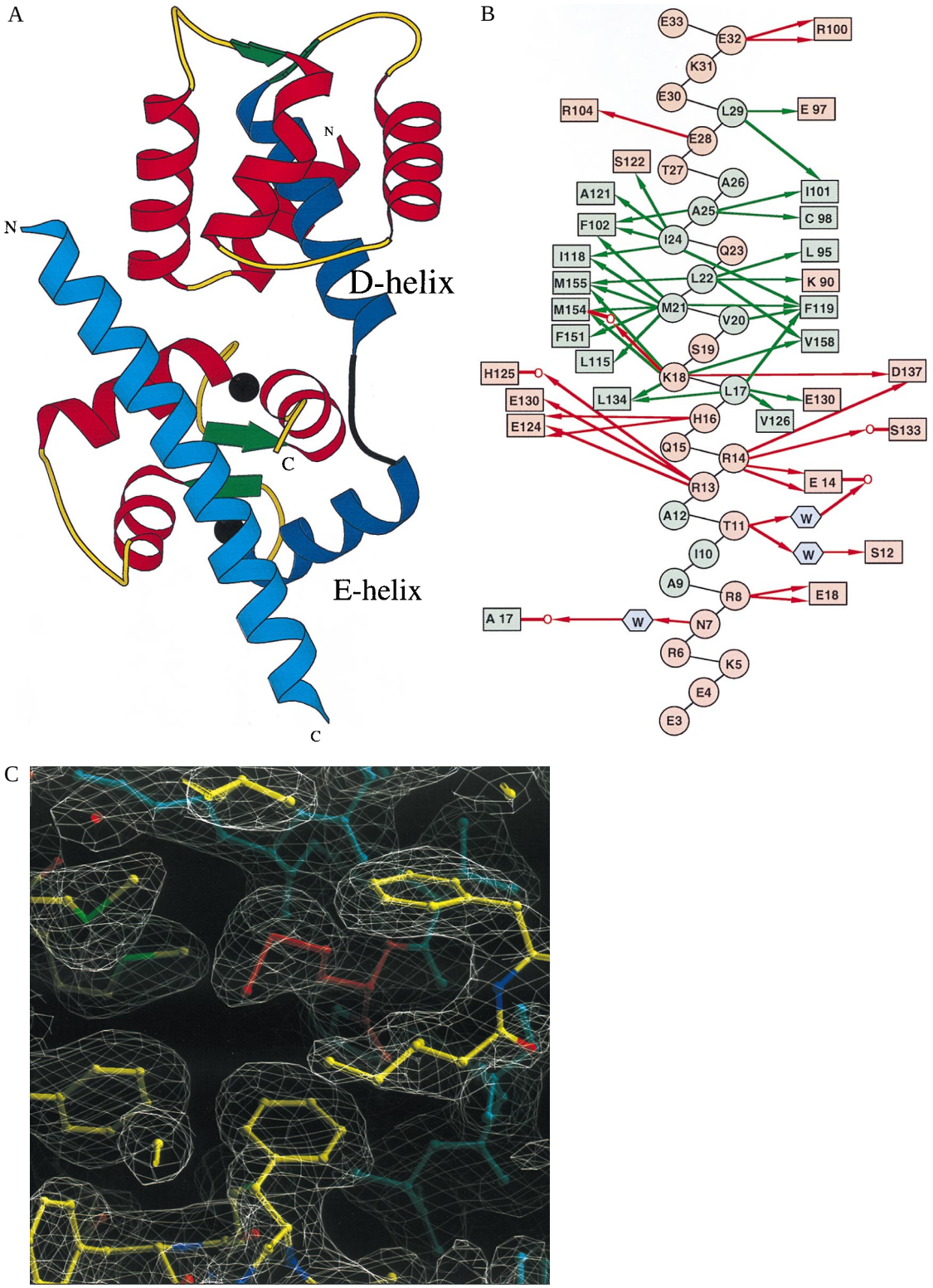

FIG. 1. Structure of the TnC/TnI$_{1-47}$ complex. (*A*) Ribbon diagram of the TnC/TnI$_{1-47}$ complex structure. The α-helices, β-strands, and loops of TnC are in red, green, and yellow, respectively. The unwound and kinked central D/E α-helix of TnC is shown in blue, and the interdomain extended linker is black. The two calcium ions in the TnC C-lobe are shown as black balls. The TnI$_{1-47}$ α-helix is in cyan. The figure was drawn with the MOLSCRIPT program (21). (*B*) Hydrophobic (green arrows) and polar (red arrows) side-chain interactions between TnI$_{1-47}$ (circles) and TnC (rectangles) residues in the TnC/TnI$_{1-47}$ complex. The hydrophobic and polar residues are shown in green and red, respectively. Water molecules are shown as cyan hexagons. Main chain carbonyl oxygens of the interacting amino acids are shown as a red O attached to the subsequent residues. (*C*) Portion of the final (2Fo-Fc) electron density map and the TnC/TnI$_{1-47}$ model (ball and stick) in the hydrophobic cavity of the C-lobe of TnC. The TnI and TnC residues are shown in cyan and atom-dependent (C, N, O, and S are yellow, blue, red, and green, respectively) colors, respectively. Met-21, protruding into hydrophobic cleft of TnC, is colored red. The figure was produced with the O program (19).

structure. Thus, the conformation of each TnC lobe itself in the TnC/TnI$_{1-47}$ complex is very similar to that in the TnC$_{free}$ structure. The rms deviations between all C$_\alpha$ atoms of TnC$_{free}$ and TnC in the TnC/TnI$_{1-47}$ complex are 1.0 Å and

1.2 Å for the N- (residues 2–86) and C-lobes (residues 92–159), respectively. Among these, four C-terminal residues exhibit largest rms deviations of 6.5 Å. In the TnC/TnI_{1-47} complex, these residues are moved into a close proximity with TnI_{1-47} α-helix.

The TnI_{1-47} fragment in the TnC/TnI_{1-47} complex contains a 31-residue long α-helix that is slightly bent toward the concave surface of the TnC molecule (Fig. 1*A*). Fourteen residues at the C-end of TnI_{1-47} are disordered in the crystal, and probably do not have contacts with TnC. The TnI_{1-47} α-helix makes multiple polar and van der Waals interactions with both lobes of TnC. According to these interactions, the TnI_{1-47} α-helix may be divided into two parts. The N-terminal (residues 3–12) and C-terminal (residues 13–33) portions of this α-helix are bound to the N- and C-lobes of TnC, respectively. Arg-14 of TnI_{1-47} is located at the interface between the lobes of TnC and bridges them by four strong hydrogen bonds (Fig. 1*B*). The C-terminal part of the TnI α-helix is tightly bound to the C-lobe of TnC by 11 hydrogen bonds. In addition, there are 38 van der Waals interactions (<4 Å) between the amphiphilic C-end of TnI_{1-47} α-helix and the TnC residues in the hydrophobic pocket of the C-lobe (Fig. 1*B*). Thus, the hydrophobic residues of TnI_{1-47} and TnC complement each other and constitute the hydrophobic core of the TnC/TnI_{1-47} complex. We believe that these hydrophobic interactions play a major role in the recognition between TnC and TnI_{1-47}. It is worthwhile to mention that Met-21 of TnI_{1-47} seems to be of central importance for the recognition; its bulky side chain protrudes deeply into the hydrophobic cavity of the TnC C-lobe and makes a total of eight van der Waals contacts with the TnC residues (Fig. 1 *B* and *C*). Judging by the crystal structure, the interactions of TnI_{1-47} with the N-lobe of TnC seem to be weaker than those with the C-lobe. There are only four direct and three water-mediated hydrogen bonds (Fig. 1*B*). It is likely that these interactions are required mostly to anchor the TnC N-lobe to TnI, to stabilize the compact conformation of TnC, and do not play an essential role in recognition.

Comparison with Calmodulin. The overall conformation of TnC and the rearrangement of the TnC lobes induced by TnC/TnI_{1-47} complex formation resemble another Ca^{2+}-receptor protein, calmodulin, in the complexes with its target peptides (22, 23). The extended dumb-bell shaped molecules of both proteins undergo substantial conformational changes on binding to other proteins. In both cases, the dramatic reorientation of the lobes accompanies the unwinding and the kink of the central connecting α-helix, resulting in the compact globular protein structure. Moreover, the target peptides of both proteins adopt α-helical conformations, and the recognition mechanism involves multiple hydrophobic interactions between the proteins and the amphiphilic portions of the bound peptides. The latter feature also resembles the binding between the myosin light and heavy chains (24). However, there is an essential difference between TnC and calmodulin (myosin light chain) in the mode of binding to the substrates. In the calmodulin/peptide complexes, the hydrophobic binding sites of both lobes are turned toward each other and toward the center of the molecule. This orientation allows both lobes of calmodulin to interact simultaneously with two regions of the same target α-helix. In contrast, in the TnC/TnI_{1-47} complex, the hydrophobic pockets in the C- and N-lobes are turned out of the molecular center and are located on opposite sides of the molecular surface. If TnC in the functional Tn adopts the conformation observed in the TnC/TnI_{1-47} complex, the binding of a single α-helix to both lobes of TnC, as in the calmodulin complexes, is impossible.

Regulatory Segment of TnI. The understanding of how the inhibition of acto-myosin ATPase is released is of central importance in the studies of mechanism of regulation of muscle contraction. Therefore, in the past years many biochemical and biophysical studies were focused on the inhibitory segment (residues 96–116) of TnI (5, 25). The inhibitory segment was shown to bind to either actin-tropomyosin or TnC, thus switching on and off the acto-myosin ATPase activity (6–8). On the other hand, the conformational changes between "closed" and "open" forms of TnC regulatory N-lobe induced by Ca^{2+} binding also entail the regulation of muscle contraction. The C- and N-lobes of TnC are very similar in both sequence and structure in the Ca^{2+}-bound states (9–11, 26). Thus, the TnC/TnI_{1-47} structure suggests that "open" N-lobe of TnC would bind to another amphiphilic α-helix in a symmetrical manner. In view of important regulatory role of TnI inhibitory segment, it is likely that this α-helix is located in the vicinity of the inhibitory peptide in TnI. Indeed, such a hydrophobic segment exists at the C-end of the TnI inhibitory sequence and was predicted to have an α-helical conformation (27). This region is highly conserved among TnIs from different species. The N-terminal and "inhibitory" sequences are similar in the general hydrophobicity of the amino acids, although the sequence identity is low (Fig. 2). However, the methionine residue (Met-121), corresponding to the N-terminal Met-21, which was proposed to play an important role in the recognition between TnC and TnI_{1-47}, is conserved in the "inhibitory" sequence (Fig. 2). The measurements of the binding constants of two TnI inhibitory fragments to TnC showed that TnI_{96-116} preferably interacts with the C-lobe of TnC, whereas its C-terminal extension, TnI_{96-148}, is most tightly bound to the TnC N-lobe (27). At a high Ca^{2+} concentration, the segment at the C-end of the TnI inhibitory sequence was protected against proteolysis (28) and was proved to be crucial for the regulatory activity of Tn (29). Taken together, the biochemical data and our hypothesis strongly suggest that the TnI inhibitory region could be extended to the regulatory TnI fragment (TnI_{reg}, residues 96–127 of TnI) (Fig. 2), in which the amphiphilic C-end (residues 117–127) would play the major regulatory role in the relief of the inhibition of the actomyosin Mg^{2+}-ATPase, through binding to the hydrophobic pocket of the TnC N-lobe in its "open" state.

Model Building of TnI_{reg}. The three-dimensional model of the TnC/TnI_{reg} complex (Fig. 3*A*) was constructed in four steps. First, the "closed" N-lobe of TnC in the TnC/TnI_{1-47} complex was replaced by a Ca^{2+} bound, "open" N-lobe (Protein Data Bank entry 1TNQ) (26). Second, the C-lobe bound to the TnI_{1-47} α-helix was superimposed on the "open" N-lobe, and the resulting orientation of the α-helix was taken as a starting model for TnI_{reg}. Third, the TnI_{1-47} sequence was replaced by that of TnI_{reg} in the model. At this stage, the conserved Met-121 of TnI_{reg} fits very well into the hydrophobic cleft of the N-lobe of TnC (Fig. 3*B*). Finally, a two-proline kink

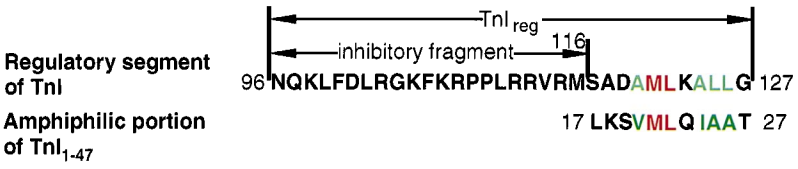

FIG. 2. TnI sequence at the C-end (residues 117–127, rabbit skeletal muscle) of the inhibitory fragment (residues 96–116) aligned with the amphiphilic portion of TnI_{1-47}. The identical residues are red, the distinct residues are black, and the amphiphilic residues corresponding to the hydrophobic amino acids are green.

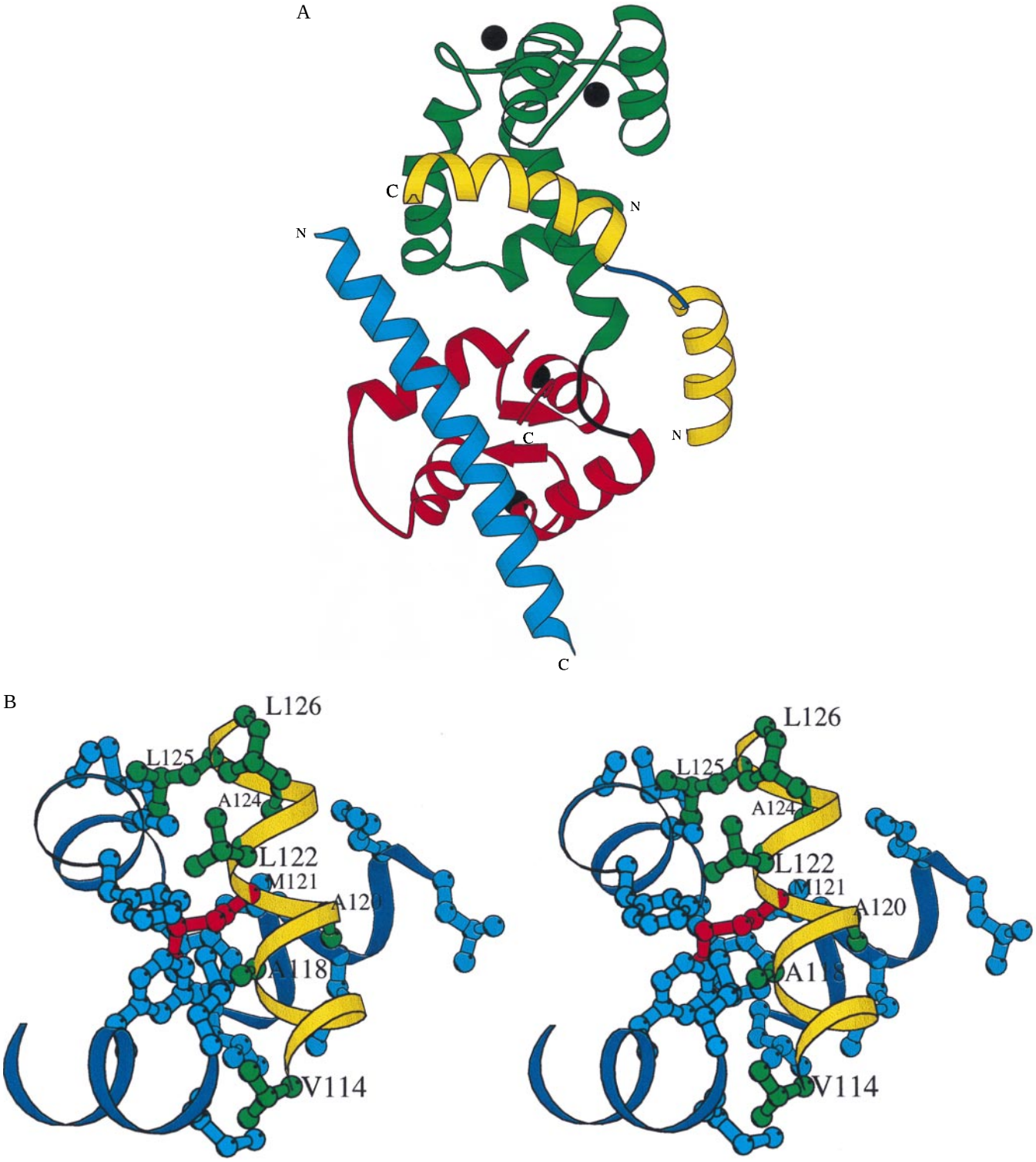

FIG. 3. TnC/TnI_{reg} model structure. The figure was prepared by using MOLSCRIPT (21). (*A*) Ribbon diagram of the TnC/$TnI_{1–47}$/TnI_{reg} model. The two "open" N- and C-lobes of TnC are green and red, respectively. Four calcium ions are shown as black balls. The $TnI_{1–47}$ and TnI_{reg} α-helices are shown in cyan and yellow, respectively. The two-proline linker (Pro-109 and Pro-110) in the TnI_{reg} α-helix is shown in blue. (*B*) Stereo view of the hydrophobic core of the TnC/TnI_{reg} model structure. The TnC and TnI_{reg} α-helices are shown in blue and yellow, respectively. The side chains of the residues in the hydrophobic pocket of the "open" C-lobe of TnC and the complementary hydrophobic residues of TnI_{reg} (ball and stick) are cyan and green, respectively. Protruding side chain of Met-121 is shown in red.

(residues 109–110) was introduced in the TnI_{reg} α-helix, on the basis of an NMR structure of the inhibitory peptide (residues 104–115) bound to TnC (30) (Table 2). In addition, the N-end of the α-helix was extended to the TnI residue 96 to make it more consistent with the biochemical data. The model was then refined by energy minimization with the X-PLOR program (17). At the high Ca^{2+}-concentration, the distances between Trp-106 (TnI) and Met-25, Cys-89 (TnC) are 21.6 Å and 20.2 Å, respectively, which are in good agreement with the respective distances of 24.2 Å and 23.2 Å measured from the proposed model of the TnI_{reg} bound to open TnC N-domain (X. Zhao, T. Kobayashi, H. Malak, I.

Table 2. Comparison of the TnC/TnI_{reg} model with NMR structure of TnI inhibitory peptide (residues 104-116) bound to TnC

Residue (TnI)	Main chain torsion angles (ϕ, ψ)			
	NMR structure		TnC/TnI_{reg} model	
	ϕ(°)	ψ(°)	ϕ(°)	ψ(°)
Lys-107	−70	−25	−66	−25
Arg-108	−59	−38	−44	−34
Pro-109	−80	174	−58	149
Pro-110	−78	161	−89	152
Leu-111	−59	−23	−56	−26
Arg-112	−66	−43	−55	−38

Gryczynski, J. Lakowicz, R. Wade, and J. H. Collins, personal communication).

The TnI_{reg} model could be divided into two parts; the N-terminal part (residues 96–107) is likely to interact with the C-lobe of TnC, whereas the C-terminal region (residues 108–127) is strongly bound to the TnC N-lobe (Fig. 3*A*). In the TnC/TnI_{reg} model, seven hydrophobic residues at the C-terminal region of TnI_{reg} are likely to interact with the 13 TnC residues in the hydrophobic cavity of the N-lobe (Fig. 3*B*). Interestingly, according to our model, Phe-100 of TnI_{reg} may form multiple hydrophobic contacts with Phe-148 and Leu-152 of TnC, which would increase the affinity of TnI_{reg} to the TnC C-lobe.

Implications for the Regulation of Muscle Contraction. The TnC/TnI_{reg} model suggests the possible mechanism of regulation of muscle contraction by Tn complex. At the binding of Ca^{2+} the conformation of regulatory N-lobe of TnC will be changed from the "closed" to "open" state. This structural transformation of TnC probably would facilitate the relief of inhibition of actomyosin ATPase by TnI_{reg}. Thus, TnI_{reg} preferably would bind to TnC, and its amphiphilic C-end would be locked in the hydrophobic cavity of TnC N-lobe through the multiple van der Waals interactions. The release of Ca^{2+} from N-lobe of TnC would initiate its transformation to the "closed" form, which would push the amphiphilic α-helix of TnI_{reg} out of the pocket. After "closing" of TnC N-lobe this hydrophobic α-helix could not bind on the surface of TnC covered by hydrophilic residues. Thus, the amphiphilic TnI_{reg} α-helix would be able to bind to some putative hydrophobic site in the actin molecule, which increases the affinity of TnI_{reg} to actin, and facilitates its release from TnC and the binding to actin-tropomyosin.

CONCLUSIONS

The TnC/$TnI_{1–47}$ complex structure and the TnC/TnI_{reg} model provide several important implications. (*i*) Within Tn, the TnC molecule has a compact globular shape with direct polar interactions between the N- and C-lobes. (*ii*) The N-terminal region of TnI and TnI_{reg} have α-helical structures and are bound to TnC in a pseudo-symmetrical manner. (*iii*) The recognition of $TnI_{1–47}$ and TnI_{reg} by TnC is accomplished by hydrophobic interactions, in which Met-21 ($TnI_{1–47}$) and Met-121 (TnI_{reg}) are probably the key residues. (*iv*) TnI_{reg} binds to both lobes of TnC in the presence of Ca^{2+}, and hence, it alone may induce the functional, compact conformation of TnC. Consistent with this, an N-terminal deletion mutant, $TnI_{58–182}$, still can constitute a functional Tn, but only at high Ca^{2+} concentrations (31). (*v*) The two-proline kink in the TnI_{reg} α-helix probably is required to direct the N-end of TnI_{reg} toward the TnC C-lobe. (*vi*) The difference between calmodulin and TnC in the binding to their targets accounts for their distinct biological functions. Calmodulin functions as an isolated protein; thus, both of its lobes are involved in signal transduction. In contrast, TnC is integrated into the Tn complex through its C-lobe, and only the N-lobe possesses regulatory activity.

In conclusion, the binding of $TnI_{1–47}$ to the TnC C-lobe is likely to play a primarily structural role in the formation of Tn, whereas the amphiphilic C-end of TnI_{reg} forms the actual switch that moves between actin-tropomyosin and the hydrophobic cleft of the N-lobe of TnC in a Ca^{2+}-dependent manner, thereby regulating the process of muscle contraction.

We thank Yumiko Saijo for preparing the crystals, A. Thompson, V. Stojanoff, and M. Yao for help at the beam-line BM14, K. Imada for help using the laboratory x-ray system, and J.H. Collins for letting us refer to unpublished results. We are grateful to I. Ohtsuki, S. Cusack, and Susan Tsutakawa for reviewing the manuscript before submission, and to F. Oosawa, S. Ebashi, and T. Nitta for helpful discussions and encouragement.

1. Ebashi, S. & Endo, M. (1968) *Prog. Biophys. Mol. Biol.* **18,** 123–183.
2. Ebashi, S., Endo, M. & Ohtsuki, I. (1969) *Q. Rev. Biophys.* **2,** 351–384.
3. Lehrer, S. S. (1994) *J. Muscle Res. Cell Motil.* **15,** 232–236.
4. Ohtsuki, I., Maruyama, K. & Ebashi, S. (1986) *Adv. Protein Chem.* **38,** 1–67.
5. Zot, A. S. & Potter, J. D. (1987) *Annu. Rev. Biophys. Biophys. Chem.* **16,** 535–559.
6. Potter, J. D. & Gergely, J. (1974) *Biochemistry* **13,** 2697–2703.
7. Tao, T., Gong, B. J. & Leavis, P. C. (1990) *Science* **247,** 1339–1341.
8. Miki, M. (1990) *Eur. J. Biochem.* **187,** 155–162.
9. Herzberg, O., Moult, J. & James, M. N. (1986) *J. Biol. Chem.* **261,** 2638–2644.
10. Strynadka, N. C., Cherney, M., Sielecki, A. R., Li, M. X., Smillie, L. B. & James, M. N. (1997) *J. Mol. Biol.* **273,** 238–255.
11. Houdusse, A., Love, M. L., Dominguez, R., Grabarek, Z. & Cohen, C. (1997) *Structure* **5,** 1695–1711.
12. Herzberg, O. & James, M. N. (1985) *Nature (London)* **313,** 653–659.
13. Sundaralingam, M., Bergstrom, R., Strasburg, G., Rao, S. T., Roychowdhury, P., Greaser, M. & Wang, B. C. (1985) *Science* **227,** 945–948.
14. Saijo, Y., Takeda, S., Scherer, A., Kobayashi, T., Maéda, Y., Taniguchi, H., Yao, M. & Wakatsuki, S. (1997) *Protein Sci.* **6,** 916–918.
15. Otwinowski, Z. & Minor, W. (1997) in *Methods in Enzymology*, eds. Carter, C. W. J. & Sweet, R. M. (Academic, San Diego), pp. 307–326.
16. Collaborative Computational Project No 4 (1994) *Acta Crystallogr. D* **50,** 760–763.
17. Brünger, A. (1992) X-PLOR Version 3.1 Manual (Yale Univ. Press, New Haven).
18. Otwinowski, Z. (1993) in *Proceedings of the CCP4 Study Weekend*, eds. Sawyer, N. I. L. & Borley, S. (SERC Daresbury, Daresbury, U.K.), pp. 56–62.
19. Jones, T. A., Zou, J. Y., Cowan, S. E. & Kjeldgaard, M. (1991) *Acta Crystallogr. A* **47,** 110–119.
20. Laskowski, R. A., MacArthur, M. W., Moss, D. S. & Thornton, J. M. (1993) *J. Appl. Cryst.* **26,** 283–291.
21. Kraulis, P. J. (1991) *J. Appl. Cryst.* **24,** 946–950.
22. Ikura, M., Clore, G. M., Gronenborn, A. M., Zhu, G., Klee, C. B. & Bax, A. (1992) *Science* **256,** 632–638.
23. Meador, W. E., Means, A. R. & Quiocho, F. A. (1993) *Science* **262,** 1718–1721.
24. Xie, X., Harrison, D. H., Schlichting, I., Sweet, R. M., Kalabokis, V. N., Szent-Gyorgyi, A. G. & Cohen, C. (1994) *Nature (London)* **368,** 306–312.
25. Farah, C. S. & Reinach, F. C. (1995) *FASEB. J.* **9,** 755–767.
26. Gagne, S. M., Tsuda, S., Li, M. X., Smillie, L. B. & Sykes, B. D. (1995) *Nat. Struct. Biol.* **2,** 784–789.
27. Pearlstone, J. R., Sykes, B. D. & Smillie, L. B. (1997) *Biochemistry* **36,** 7601–7606.
28. Takeda, S., Kobayashi, T., Taniguchi, H., Hayashi, H. & Maéda, Y. (1997) *Eur. J. Biochem.* **246,** 611–617.
29. Farah, C. S., Miyamoto, C. A., Ramos, C. H., da Silva, A. C., Quaggio, R. B., Fujimori, K., Smillie, L. B. & Reinach, F. C. (1994) *J. Biol. Chem.* **269,** 5230–5240.
30. Campbell, A. P. & Sykes, B. D. (1991) *J. Mol. Biol.* **222,** 405–421.
31. Potter, J. D., Sheng, Z., Pan, B.-S. & Zhao, J. (1995) *J. Biol. Chem.* **270,** 2557–2562.